Effects of POSS Particles on the Mechanical, Thermal, and Morphological Properties of PLA and Plasticised PLA

Dilek Turan,[1] Humeyra Sirin,[1] Guralp Ozkoc[2]

[1]*Department of Chemical Engineering, Kocaeli University, 41380 Kocaeli, Turkey*
[2]*Department of Polymer Science and Technology, Institute of Natural and Applied Sciences, Kocaeli University, 41380 Kocaeli, Turkey*

Received 21 September 2010; accepted 18 November 2010
DOI 10.1002/app.33802
Published online 25 February 2011 in Wiley Online Library (wileyonlinelibrary.com).

ABSTRACT: The mechanical, thermal, and morphological properties of melt compounded aminopropylisobutyl-polyhedral oligomeric silsesquioxane (POSS)/poly(lactic acid) (PLA) and poly(ethylene glycol) (PEG)-plasticized PLA composites were investigated. It was found that the addition of POSS to the PLA reduced the melt viscosity of the composites acting as a lubricating agent. Dynamic mechanical analysis and tensile tests showed that the modulus and elongation at break values improved at low (1% and 3%) POSS loading levels. Scanning electron microscopy observation indicated that POSS particles were well dispersed in both PLA and plasticized PLA. The interfacial interaction of POSS with the polymer matrix was found to be better in the presence of plasticizer. The presence of POSS also affected the thermal properties of the PLA and plasticized PLA. It was revealed from DSC that POSS particles acted as a nucleating agent for PLA. Moreover, the percent crystallinity was found to be higher in the presence of POSS for both PLA and plasticized PLA. © 2011 Wiley Periodicals, Inc. J Appl Polym Sci 121: 1067–1075, 2011

Key words: PLA; POSS; composite; compounding; mechanical properties

INTRODUCTION

Modernization of the life leads to increase of plastic consumption rates, which become a long-term solid waste problem. Compostable and biodegradable polymeric materials offer useful solution to solid waste management issues. Poly(lactic acid) (PLA) is a linear, semicrystalline, aliphatic, biodegradable polyester that can be produced from lactic acid by the fermentation of renewable sources such as whey, corn, potato, or molasses. PLA is a brittle polymeric material and mostly plasticized before using. The potential plasticizers for PLA are citrate esters, poly(ethylene glycol) (PEG), glucose monoesters, glycerol, and oligomeric lactic acid.[1] These additives improve the ductility and the process-ability of the PLA. However, it is more important to balance the stiffness and the flexibility of the packaging films. The development of composites has improved the possibility of enhancing mechanical properties of polymeric materials without losing ductility, in contrast to typical property trade-offs seen in conventional composites.[2]

Correspondence to: G. Ozkoc (guralp.ozkoc@kocaeli.edu.tr).

Contract grant sponsor: KOU-BAP Project; contract grant number: 2010/84.

Polyhedral oligomeric silsesquioxanes (POSS) are useful candidates for reinforcement of polymers.[2–10] POSS are structurally cage-like molecules with chemical formula of $(RSiO_{1.5})_n$. The R groups are responsible from solubility and compatibility of the POSS with other polymers. It is possible to modify the reactivity by changing these groups through organo-chemical modification. A POSS molecule of 1.5 nm size leads to make it comparable with most of the polymer dimensions.[3] The incorporation of POSS containing reactive groups into a polymer matrix creates a possible nanoscale reinforcement, in which POSS are linked to polymer chains covalently. There is limited number of work published in the literature dealing with PLA/POSS composites. Zhaobin and Hong investigated the dynamic mechanical properties, crystallization and hydrolytic degradation of solution casted octaisobutyl-POSS reinforced PLA composites.[4] It was shown that the POSS particles were well dispersed in PLA matrix around 200–400 nm level. The modulus of PLA matrix was improved by the incorporation of POSS. Besides, it was reported that the addition of the POSS to the PLA matrix accelerated the crystallization process acting as a heterogeneous nucleating agent. Wang et al. studied on melt compounded epoxycyclohexyl-POSS (ePOSS) or octavinyl-POSS (vPOSS) with PLA/Poly(butylene succinate-*co*-adipate) blends.[5] The X-ray diffraction (XRD) analysis showed that ePOSS dispersed uniformly, but vPOSS stayed in the

crystalline state in the matrix after processing. The chemical bonding between ePOSS and the PLA/PBSA was shown by FTIR analysis. The added value of ePOSS on the mechanical properties was found to be better than that of vPOSS. In a most recent work, L-lactide tethered 3-hydroxypropylheptaizobutyl-POSS was used in ring-opening polymerization of L-lactide in the presence of a catalyst.[6] Authors proved by H-NMR that POSS-PLA hybrids acted as an initiator in the polymerization reaction. The dispersion of POSS molecules in the matrix was found to be well without forming any crystallization aggregates, observed by XRD. The researchers also used POSS-PLA hybrid as nanoscale reinforcement for PLA at 1–30 wt %. They observed that the thermo-oxidative stability of the composites improved in the presence of POSS-PLA hybrids. Other than PLA/POSS composites, there are studies published in the literature dealing with preparation, properties, and application of thermoplastics-based composites.[7–14] In general, the common results revealed from these studies are enhanced service temperatures, improved modules, and improved crystallization of polymer/POSS composite system.

In this study, it is aimed to investigate the effects of amine functionalized POSS on the mechanical and thermal properties and morphology of PLA and plasticised PLA. The reason of choosing amine functionality is its potential of making covalent bonding with the —COOH end group of PLA. The plasticizer is PEG. Its ratio in the PLA is kept constant at 20 wt %. The POSS content was varied as 1, 3, and 10 wt %. The composites were prepared in a laboratory twin screw compounder to mimic the industrial melt compounding process.

EXPERIMENTAL

Materials

Poly(lactic acid) (PLA 2002D, extrusion grade, MFI: 5–7 g/10 min at 210°C, 2.16 kg) was provided by Cargill-Dow. Poly(ethylene glycol) (PEG, MW = 8000 g/moles) (Sigma–Aldrich) was used as the plasticizer. The aminopropylisobutyl-POSS was purchased from Hybrid Plastics. It was a white crystalline powder. It is soluble in THF and chloroform that are also solvents for PLA. Therefore, it is expected to have miscibility between POSS and PLA. The chemical structure of POSS is shown in Figure 1.

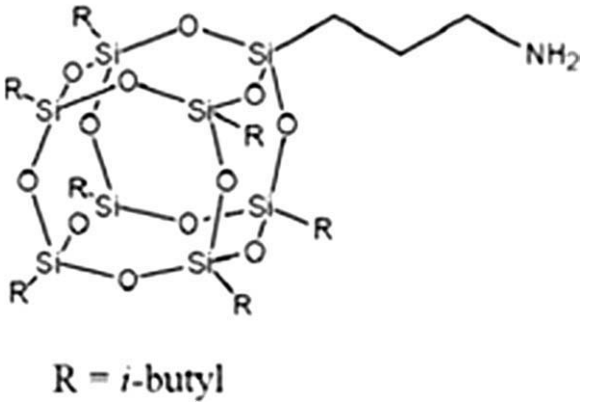

Figure 1 The chemical structure of aminopropylisobutyl-POSS (R: i-butyl group).

Microcompounding and microinjection molding

A total of 1, 3, and 10 wt % POSS including PLA and PLA/PEG mixtures were prepared. To make a comparison, neat PLA and neat PLA/PEG were also prepared. The materials were dry-mixed at predefined amounts before processing. The mixture was melt compounded in a twin-screw microcompounder (15 mL Microcompounder, DSM Xplore). The screw speed was 100 rpm and barrel temperature was 200°C. The mixing time was kept constant at 3 min. At the end of this period, the extrudate was taken by changing the position of the valve to guide the polymer to the die. Molten compound was subsequently injection molded using a DSM Xplore 10 mL injection molding machine to obtain ISO 527-2/5A tensile bars and ISO 180 bars. The injection and holding pressures were set to 10 bars. Melt temperature and mold temperature were 200°C and 25°C, respectively.

Vertical force measurements

The barrel of the microcompounder is positioned on a lever, which swivels around a stationary axis and counter balanced by a load-cell at the other end. A detailed picture of the schematic picture of vertical force measurement was given elsewhere.[15] The load-cell is 10 kN in range and measures the vertical force exerted by the barrel opposing the pushing forces imposed by the screws toward the bottom, while the polymer melt is pumped through the recirculation channel or die. For a given polymer, if the screw speed and the barrel temperature are fixed, then the vertical force can be used as a representation of melt viscosity of the polymer. In this study, the vertical force measurement is conducted to compare the melt viscosity of the materials processed as a function of composition. The vertical force data are recorded in every minute after feeding.

Tensile test and dynamic mechanical analysis

Tensile tests were performed on injection molded dog-bone samples according to ISO 527-2-5a using a Schimatzu EZ Servey universal testing machine. The

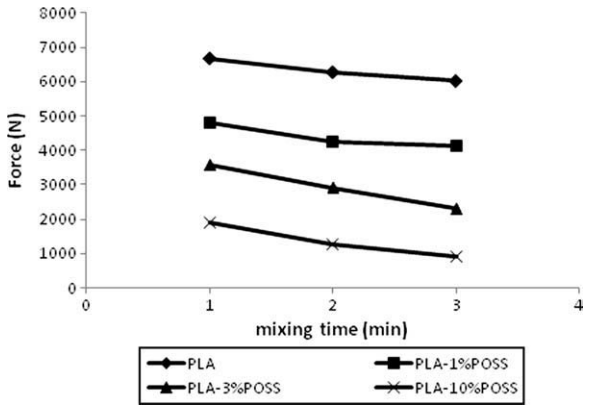

Figure 2 The variation of vertical force (N) with respect to POSS content in PLA–POSS composites.

crosshead speed was 5 mm/min. The average results of 5 replications were reported. Dynamic mechanical analyses (DMA) were conducted on TA Instruments Q800 model DMA tester using single beam cantilever mode at 1 Hz. The temperature range was 0–100°C; scan rate was 3°C/min.

Scanning electron microscopy

Tensile fractured surfaces of samples were observed by using JEOL JSM 6060 model scanning electron microscope. The samples were gold coated before observation to prevent arching.

Thermal analysis

Thermal properties of the polymers and polymer composites were analyzed by differential scanning calorimeter (DSC) by a Mettler Toledo DSC-1 Star model calorimeter. The analyses were conducted under N_2 atmosphere at a scan rate of 10°C/min, between 0 and 200°C. The reported values are the averages of three replications. The percent crystallinity ($\%X_c$) of the samples were calculated according to eq. (1):

$$\%X_c = \frac{\Delta H_m - \Delta H_c}{\Delta H_m^* \varphi} \times 100 \quad (1)$$

where ΔH_m is melting enthalpy (J/g), ΔH_c is cold crystallization enthalpy (J/g), ΔH_m^* is the heat of fusion for PLA (J/g), and the φ is the fraction of the polymer in the composite.

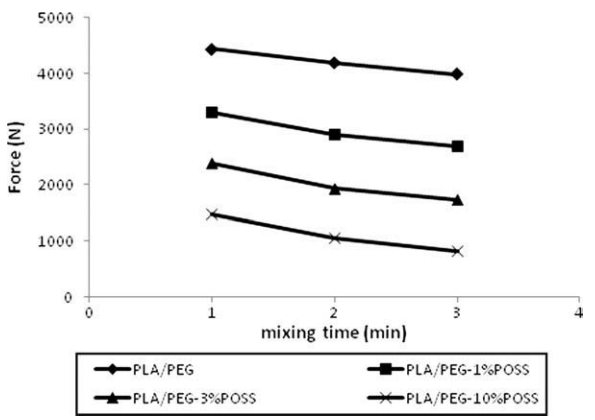

Figure 3 The variation of vertical force (N) with respect to POSS content in PLA/PEG–POSS composites.

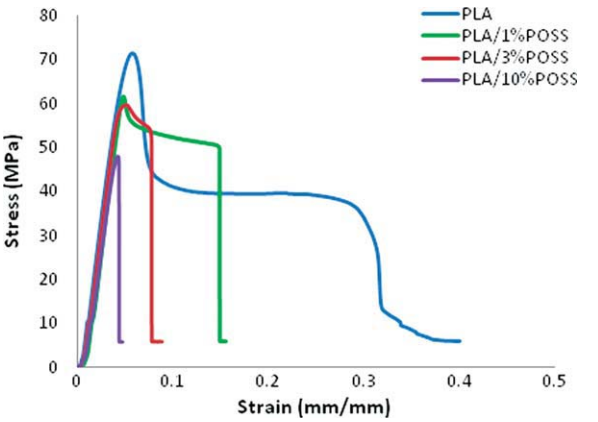

Figure 4 Representative stress–strain curves of PLA/POSS composites as a function of POSS content. [Color figure can be viewed in the online issue, which is available at wileyonlinelibrary.com.]

RESULTS AND DISCUSSIONS

Vertical force measurements

Vertical force during the extrusion was measured to judge the flow properties of the composites. Figures 2 and 3 show the variation of vertical force (N) with respect to POSS content in PLA-POSS and PLA/

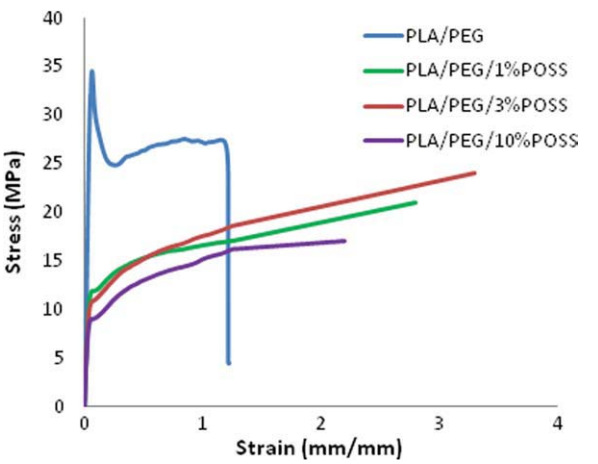

Figure 5 Representative stress–strain curves of PLA/PEG/POSS composites as a function of POSS content. [Color figure can be viewed in the online issue, which is available at wileyonlinelibrary.com.]

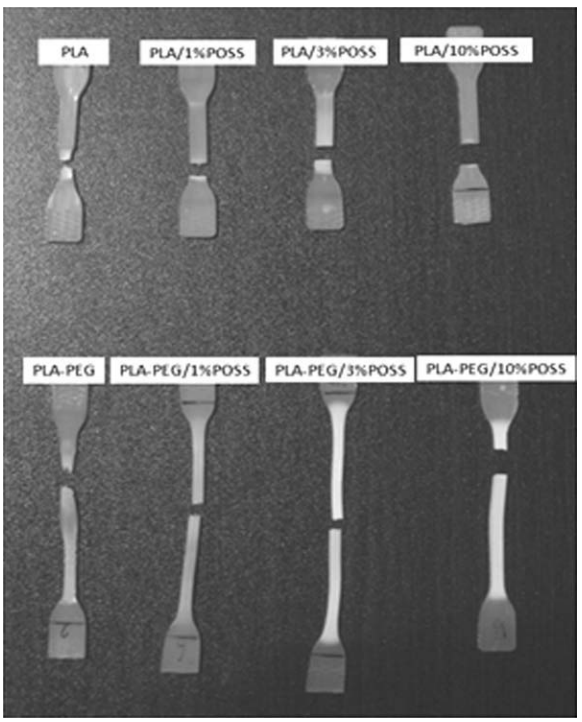

Figure 6 Representative picture of dog-bone samples after tensile test.

PEG-POSS composites, respectively. It is seen for all PLA and PLA/PEG composites that the increase in the POSS content results in a decrease in vertical force, in other words decrease in the melt viscosity of the system at any given mixing time. This can be attributed to the molecular lubricating effect of POSS particles in the polymeric matrix.[16,17] It was mentioned in the literature that the viscosity of the POSS–polymer composite depends on the level of the interaction of the constituents.[18–20] It was also explained in the literature that in the absence of a covalent bonding, the viscosity of the composite decreases with increasing POSS content; however, when the POSS is reactively bonded to the matrix, a constant increase of the viscosity with the filler content was obtained. The lowering of the viscosity can be an advantage in terms of power consumption during melt processing. When the melt viscosities of neat-PLA and neat-PLA/PEG matrices are compared, as a result of plasticization, the melt viscosity drastically decreased, as expected. The slight decrease in vertical force by the mixing time regardless of composition can be resulted from a slight decrease in molecular weight of PLA matrix despite the processing under Argon atmosphere.[21]

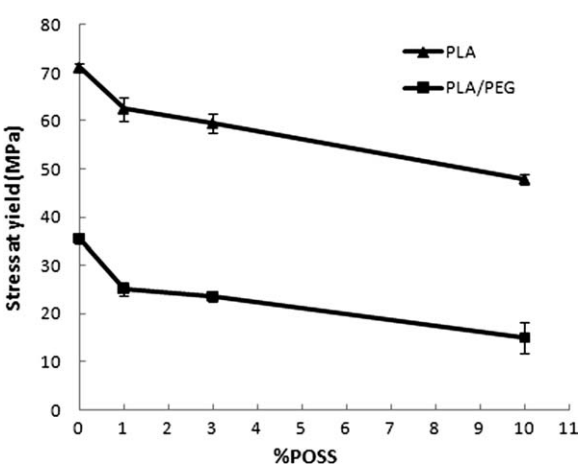

Figure 7 The variation of stress at yield values with respect to POSS content in PLA and PLA/PEG composites.

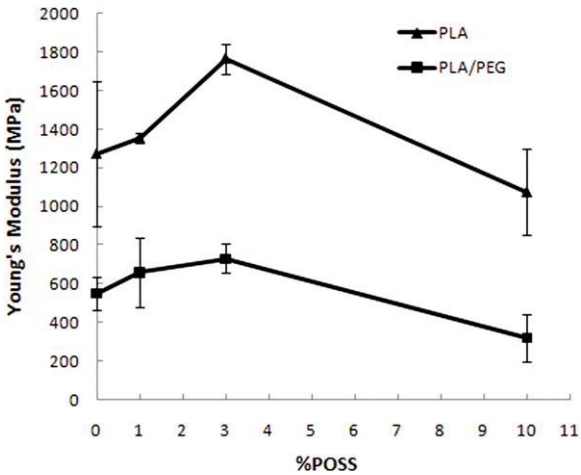

Figure 8 The variation of modulus of elasticity with respect to POSS content in PLA and PLA/PEG composites.

Tensile tests and DMA

To compare the tensile behavior of composites, representative stress–strain curves of PLA, PLA/POSS,

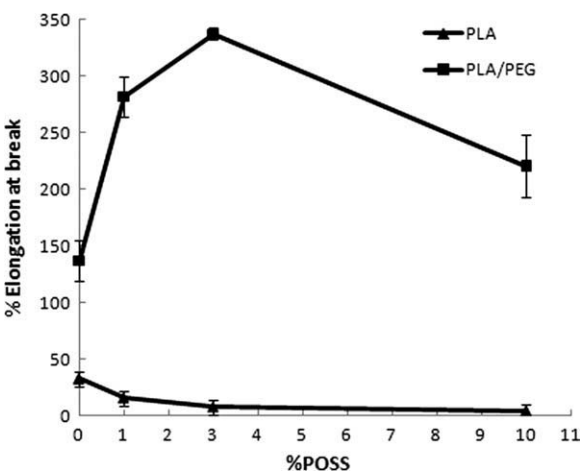

Figure 9 The variation of elongation at break values with respect to POSS content in PLA and PLA/POSS composites.

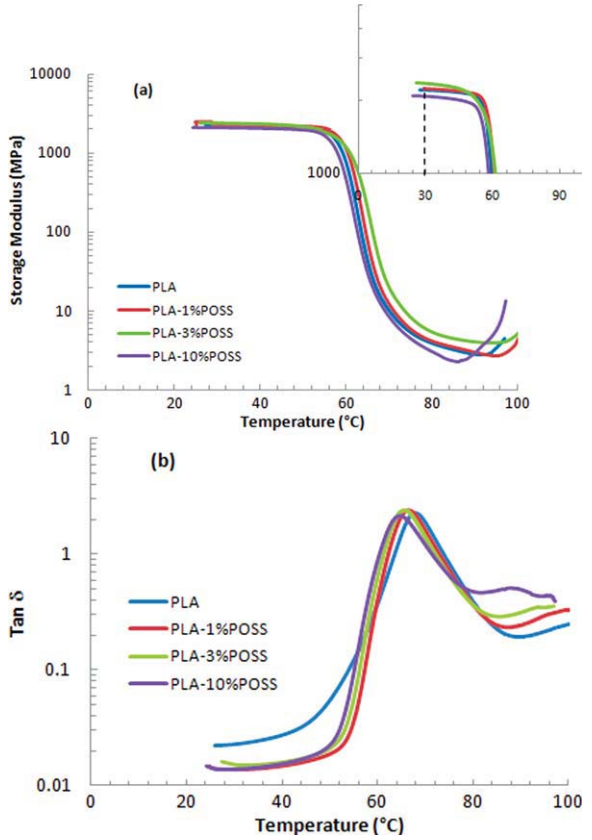

Figure 10 The variation of (a) storage modulus and (b) tan δ with respect to POSS content in PLA composites. [Color figure can be viewed in the online issue, which is available at wileyonlinelibrary.com.]

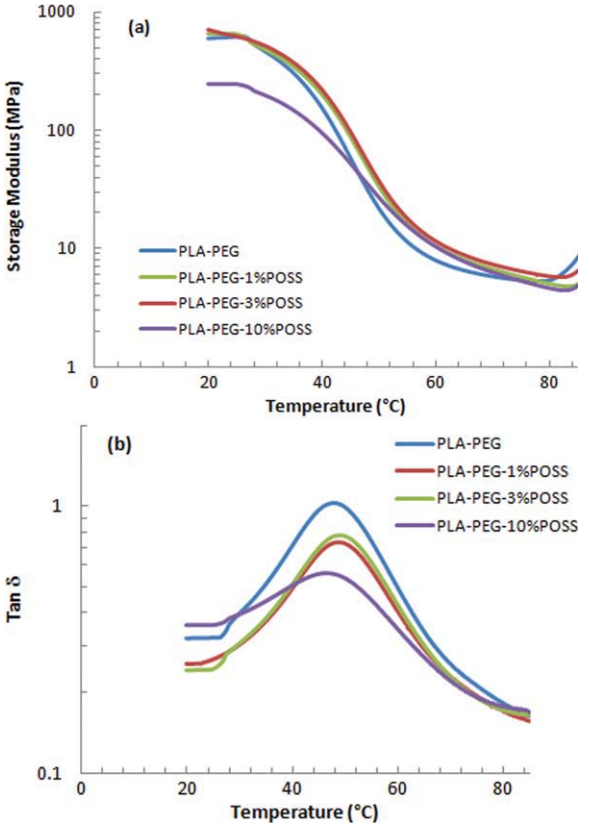

Figure 11 The variation of (a) storage modulus and (b) tan δ with respect to POSS content in PLA/PEG composites. [Color figure can be viewed in the online issue, which is available at wileyonlinelibrary.com.]

PLA/PEG, and PLA/PEG/POSS composites are given in Figures 4 and 5, respectively. Moreover, the representative pictures of tensile specimens after testing are given in Figure 6. It is seen that neat-PLA, a semicrystalline polymer, showed a yielding followed by a remarkable cold drawing before failure (Fig. 4). A necking was also visible in PLA samples seen in Figure 6. Incorporation of POSS nanoparticles to the PLA gradually reduced the strain at break and yield point. For PLA/10%POSS, the failure occurred before yield point. Any necking was observed in PLA/POSS samples (Fig. 6). In the presence of PEG (plasticizer), material showed a yielding and cold drawing before failure (Fig. 5). Plasticized PLA/POSS composites exhibited a yield point followed by a cold drawing section with strain hardening. Stress whitening is obvious in all PEG-plasticized samples during tensile test (Fig. 6).

The dependence of stress at yield, elastic modulus, and strain at break values with respect to POSS content in PLA and PLA/POSS composites is given in Figures 7–9, respectively. It is seen in Figure 7 that the incorporation of POSS to either PLA or PLA/

TABLE I
The Results of Dynamic Mechanical Analysis

Material	T_g (°C) from tan δ peak	E' (MPa) at 30°C	E' (MPa) at T^a
PLA	67.85	2116	639
PLA/1%POSS	67.50	2250	943
PLA/3%POSS	66.43	2573	1184
PLA/10%POSS	64.71	2093	439
PLA-PEG	47.85	466	153
PLA/PEG/1%POSS	48.93	483	216
PLA/PEG/3%POSS	48.57	512	256
PLA/PEG/10%POSS	47.50	199	95

[a] T is 60°C for PLA and at 40°C for PLA/PEG composites.

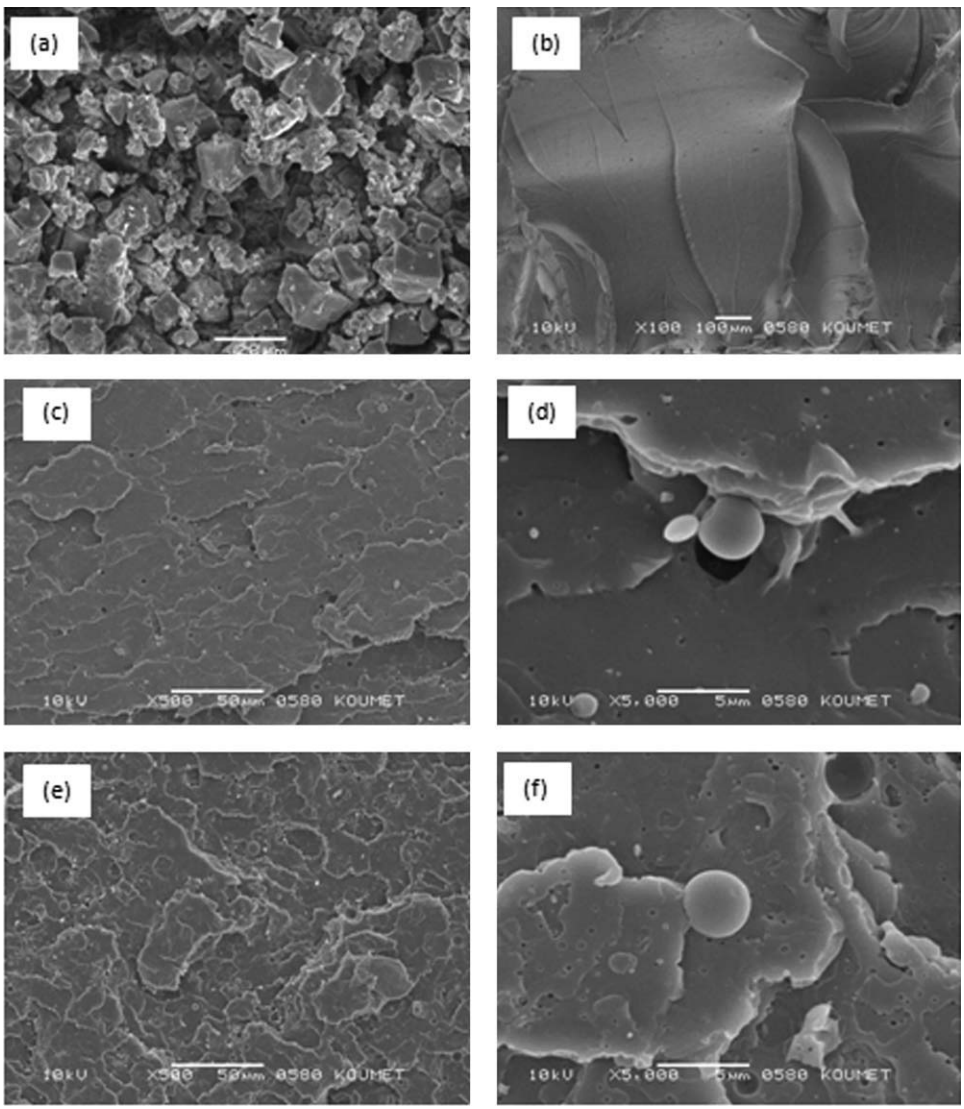

Figure 12 SEM micrographs of (a) amino-POSS particles, (b) tensile fractured surface of PLA, (c) tensile fractured surface of PLA/3%POSS at ×500 magnification, (d) tensile fractured surface of PLA/3%POSS at ×5000 magnification, (e) tensile fractured surface of PLA/10%POSS at ×500 magnification, and (f) tensile fractured surface of PLA/10%POSS at ×5000 magnification.

PEG resulted in a decrease in the strength with increasing POSS content. The addition of 20% PEG into PLA as a plasticizer decreased the strength of PLA and PLA/POSS composites nearly 50%. The modulus of elasticity of the PLA and plasticized PLA is shown in Figure 8. The modulus of plasticized PLA is lower than that of nonplasticized PLA independent of POSS content. As the POSS content increased from 1 to 3%, the modulus increases 40% for PLA/POSS and 35% for plasticized PLA/POSS. Figure 9 shows the change of elongation at break values with respect to POSS content in PLA and PLA/PEG composites. Plasticized PLA/POSS composites had higher strain at break values with respect to nonplasticized PLA/POSS composites. In PLA/POSS composite systems, the strain at break values monotonically decreased with increasing POSS content; however in plasticized PLA/POSS composites, a peak was obtained at 3% POSS in strain at break values. The PLA/POSS and PLA/PEG/POSS composites were also evaluated by DMA. The spectra of storage modulus and loss factor (tan δ) are shown in Figures 10(a,b) and 11(a,b), and the numerical values are given in Table I.

The storage modulus curves for PLA/POSS composites are given in Figure 10(a). The storage modulus of PLA/POSS composites increased as the POSS content increased from 0 to 3% due to a possible covalent or physical (H-bonding) interaction of PLA chains with $-NH_2$ functional groups; however, further increase in POSS content to 10% reduced the storage modulus at 30°C due to possible agglomerations, which is consistent with elastic modulus data obtained in tensile testing. At 60°C, just below the

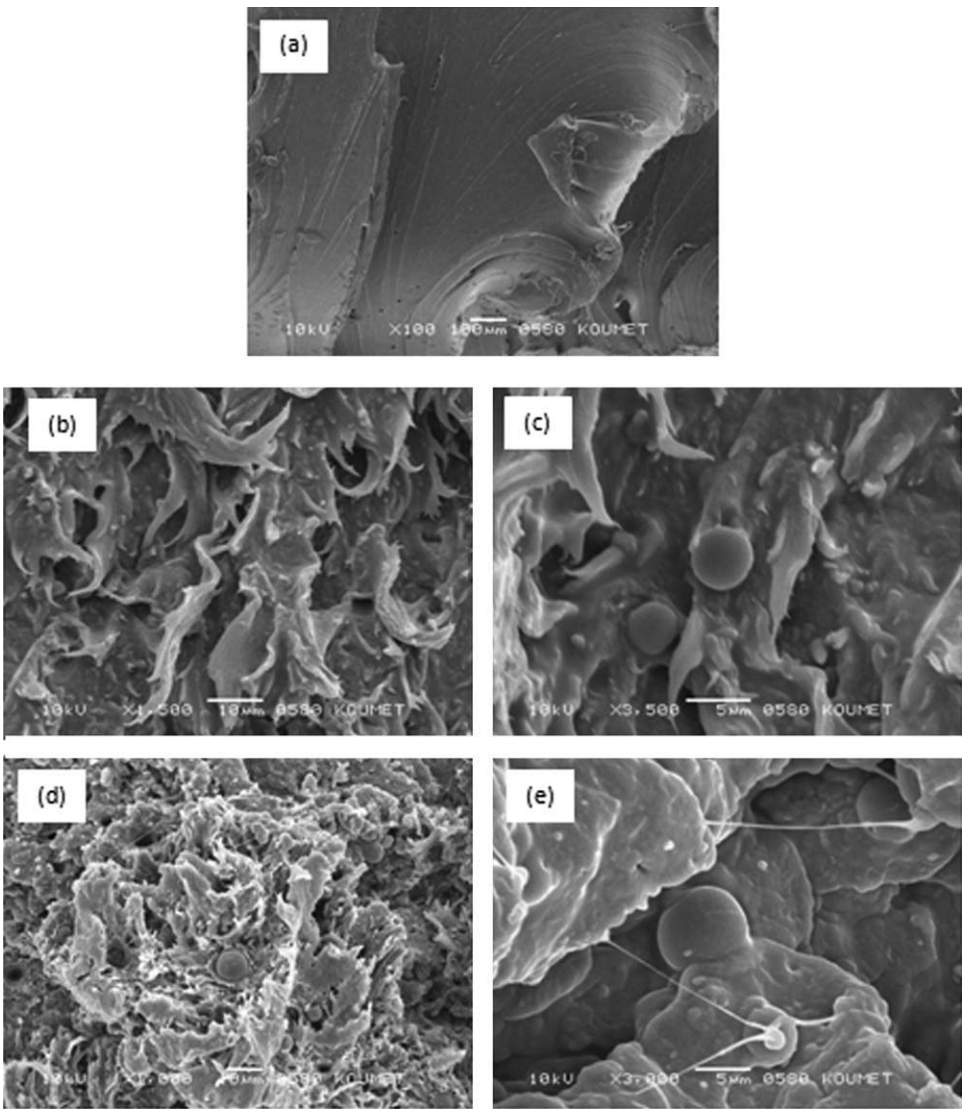

Figure 13 SEM micrograph of tensile fractured surface of (a) PLA/PEG, (b) PLA/PEG/3%POSS at ×1500 magnification, (c) PLA/PEG/3%POSS at ×3500, (d) PLA/PEG/10%POSS at ×1000 magnification, (e) PLA/PEG/10%POSS at ×3000 magnification.

T_g, the similar trend obtained at 30°C was still valid. PLA/3%POSS gave the highest storage modulus. The tan δ curves show only one peak indicating the glass transition temperature of the composites with different POSS loadings [Fig. 10(b)]. It is seen that incorporation of POSS into PLA did not make a significant change in T_g of composites at 1 and 3% loadings; however at 10%, a slight decrease was observed. PLA/PEG/POSS-based composites exhibited lower storage module values in comparison to PLA/POSS [Fig. 11(a)]. A similar trend observed in PLA/POSS was obtained also in PLA/PEG/POSS composites at both 30° and 40°C (just below the T_g). Incorporation of PEG to the neat PLA resulted in 20°C decrease in T_g due to the plasticization [Fig. 11(b)]. Addition of POSS to the plasticized PLA did not change the T_g of the composite significantly.

Morphological analysis

The morphological analysis of the POSS, PLA, PLA/POSS composites, and PLA/PEG/POSS composites was carried out by means of Scanning electron microscopy (SEM) [Fig. 12(a–f)]. The micrograph of POSS particles is given in Figure 12(a). It is seen that POSS particles have rectangular shape before compounding having an approximate particle size range of 0.5–20 μ. The tensile fractured surface of neat PLA is given in Figure 12(b). PLA fracture in brittle manner during tensile testing, which is characterized by larger cracks travel along the sample and flat regions lie between them.

The SEM micrographs of PLA/3%POSS and PLA/10%POSS composites at two different magnifications are shown in Figure 12(c,d) and (e,f), respectively. The sample surface indicates that the fracture was

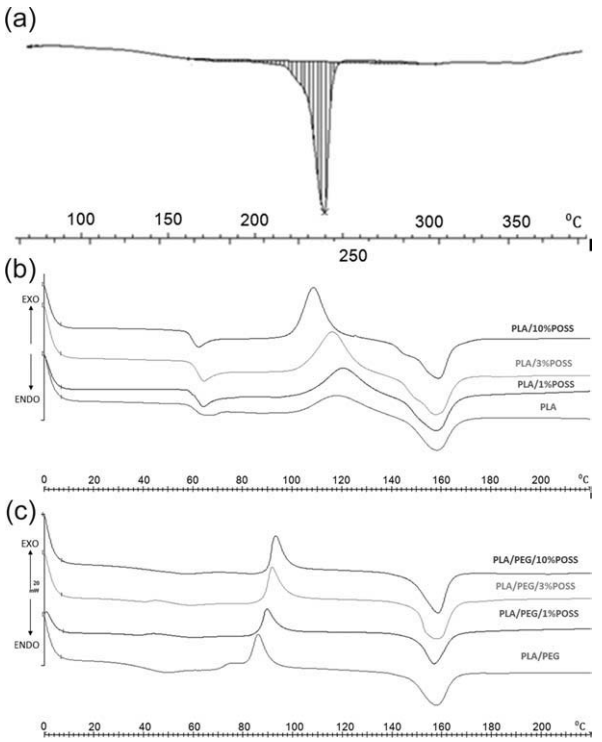

Figure 14 DSC thermogram of (a) aminopropylisobutyl-POSS, (b) PLA and PLA/POSS composites, and (c) PLA/PEG and PLA/PEG/POSS.

brittle in both 3% and 10% POSS loadings. POSS particles were identified as spherical (droplet like) particles. The formation of spheres can be attributed to melting of POSS together with PLA matrix during compounding (this will be discussed in DSC part). Most of the POSS particles detached from the PLA matrix during tensile testing resulting black empty holes. It points out a weak interface formation between amino-POSS and PLA. The POSS particles dispersed homogenously in PLA matrix. They were generally submicron-size (nanometer size); however, there are also particles at a size of 1–5 μ in 3% loading [Fig. 12(c,d)]. It can be appreciated that the number and the particle size of POSS particles increases as the concentration increases to 10% due to possible agglomeration [Fig. 12(e,f)]. The SEM micrographs of plasticized PLA and plasticized PLA/POSS composites are given in Figure 13(a–e). The fracture surface of the plasticized PLA (with 20% PEG) showed plastic deformation during tensile testing [Fig. 13(a)]. No phase separation of PEG was observed. The 3%POSS incorporated PLA/PEG samples also fractured in ductile manner [Fig. 13(b,c)]. The fibrillar morphology probably obtained due to the massive shear yielding which was the energy absorbing mechanism during tensile loading. The POSS particles in the presence of plasticizer were covered by the matrix without detaching. This can be attributed to the lower viscosity of the plasticized matrix in comparison to neat PLA, which can wet the POSS particles much easier. In 10% POSS-filled PLA/PEG, the matrix was plastically deformed as in 3%POSS. The number of POSS particles pulled-out from the matrix is higher in 10%POSS loading.

Thermal properties

The DSC thermograms of POSS, PLA, PLA/PEG, and PLA/POSS and PLA/PEG/POSS composites are shown in Figure 14(a–c); and a summary of thermograms is given in Table II. Aminopropylisobutyl-POSS is a crystalline, white powder at ambient temperature. Its DSC thermogram showed in Figure 14(a) exhibited a melting peak whose $T_{m,\text{onset}}$ was 195°C and the peak (T_m) was 240°C. Therefore, during processing at 200°C, amino-POSS is expected to be in semiliquid form, dispersed due to the shear forces exerted during compounding as droplets, seen in SEM micrographs. The difference in shape of POSS particles before and after compounding can be arised from its semiliquid form during processing.

As the T_g values obtained from DSC (Table II) is compared to the values obtained from DMA (Table I), the slightly higher T_g values of DMA is due to the frequency difference between these two measurements. PLA is characterized by a T_g at 60°C followed by an enthalpy relaxation peak. Because of the rapid cooling below T_g during injection molding process, the oriented amorphous polymer chains becomes immobile. When they are heated to their

TABLE II
DSC Results of PLA, PLA/PEG, and Their Composites

Material	T_g	T_c	T_m	$\%X_c$
PLA	60.31	117.99	157.30	21.3
1% POSS-PLA	60.94	120.36	156.95	22.3
3% POSS-PLA	61.47	115.98	156.49	30.6
10% POSS-PLA	59.89	108.53	157.81	32.5
PLA/PEG	40.69	86.00	156.82	16.9
1 %POSS-PLA/PEG	35.45	89.65	156.37	24.8
3%POSS-PLA/PEG	39.84	91.76	156.93	31.6
10%POSS-PLA/PEG	38.89	93.19	157.61	33.4

$\Delta H^*_m = 93$ J/g for PLA.[22]

T_g, they undergo a relaxation process toward an equilibrium rearranging themselves by chain segmental mobility.[23,24] A cold crystallization exotherm is appeared at 118°C and a melting endotherm at 157°C. The addition of POSS into PLA matrix did not affect the T_g of the PLA/POSS system. The enthalpy relaxation peak was still visible independently from POSS content [Fig. 14(b)]. It is of interest to emphasis that the melting peak of POSS was not present in all PLA and PLA/PEG-based composites. This indicates that POSS molecules dispersed in polymer matrix such that the crystallization of POSS molecules was suppressed. The addition of POSS molecules did not change the T_g of the resulting composite system; however, the cold crystallization temperature (T_c) of the composites was depressed by the addition of POSS. This means that POSS molecules acted as a nucleating agent for PLA crystallization.[25] The addition of 20 wt % PEG into PLA depressed the T_g of the PLA $\sim$ 20°C due to plasticization [Fig. 14(c)]. The addition of POSS did not affect the T_g of plasticized PLA; however, the cold crystallization temperature of plasticized PLA was found to be higher in the presence of POSS in the matrix, different than unplasticized PLA. This may be attributed to the possible selective interaction of POSS molecules with PEG chains, which was already observed from SEM micrographs that in the presence of PEG, matrix-POSS adhesion was better.

The degree of crystallinity of PLA was found to be about 21%. The incorporation of 1% POSS did not change this value; however, 3 and 10% addition enhanced the degree of crystallinity of PLA matrix. Incorporation of PEG into PLA decreased the percent crystallinity, but it was recovered by POSS addition to the plasticized PLA.

CONCLUSIONS

The amine functionalized POSS-reinforced PLA and plasticized PLA composites were prepared by melt compounding technique. It is observed from the SEM photos that the POSS particles well dispersed in both PLA and plasticized PLA. The interfacial interaction of POSS with the polymer matrix was better in the presence of plasticizer. It is found that the addition of POSS to the PLA reduced the melt viscosity of the composite acting as a lubricating agent. From industrial point of view, the lowering of viscosity in the presence of POSS particles can lead to a reduction in power consumption during melt compounding, which is very important. The addition of 1–3% POSS particles to the PLA and plasticized PLA improved the modulus and elongation at break values. However, further addition of POSS deteriorated the mechanical properties of the system. The presence of POSS also affected the thermal properties of PLA and plasticized PLA. It is revealed from DSC that POSS particles acted as a nucleating agent for PLA. Moreover, the percent crystallinity was found to be higher in the presence of POSS for both PLA and plasticized PLA.

The authors thank Prof. M. Zeren for allowing to use SEM facility in Department of Metallurgical and Materials Engineering of Kocaeli University and MSc. Serap Gumus for performing SEM analysis.

References

1. Pillin, I.; Montrelay, N.; Grohens, Y. Polymer 2006, 47, 4676.
2. Pinnavaia, T. J.; Beall, G. W. Polymer-Clay Composites; Wiley: New York, 2000.
3. Lichtenhan, J. D.; Schwab, J. J. Polym Prepr 2000, 41, 527.
4. Zhaobin, Q.; Hong, P. Compos Sci Technol 2010, 70, 1089.
5. Wang, R.; Wang, S.; Zhang, Y. J Appl Polym Sci 2009, 113, 3095.
6. Lee, J. H.; Jeong, G. Y. J Appl Polym Sci 2010, 115, 1039.
7. Zheng, L.; Kasi, R. M.; Farris, R. J.; Coughlin, E. B. J Polym Sci Part A: Polym Chem 2002, 40, 885.
8. Zheng, L.; Waddon, A. J.; Farris, R. J.; Coughlin, E. B. Macromolecules 2002, 35, 2375.
9. Zheng, L.; Farris, R. J.; Coughlin, E. B. Macromolecules 2001, 34, 8034.
10. Fu, B. X.; Yang, L.; Somani, R. H.; Zong, S. X.; Hsiao, B. S.; Phillips, S.; Blanski, R.; Ruth, P. J Polym Sci Part B: Polym Phys 2001, 39, 2727.
11. Zheng, L.; Kasi, R. M.; Farris, R. J.; Coughlin, E. B. Polym Mater Sci Eng Prepr 2001, 84, 114.
12. Schwab, J. J.; Reinerth, W. A., Sr.; Lichtenhan, J. D.; An, Y. Z.; Phillips, S. H.; Lee, A. Polym Prepr 2001, 42, 48.
13. Zheng, L.; Farris, R. J.; Coughlin, E. B. J Polym Sci Part A: Polym Chem 2001, 39, 2920.
14. Xiao, J.; Feher, F. J. Polym Prepr 2002, 43, 504.
15. Ozkoc, G.; Bayram, G.; Quaedflieg, M. J Appl Polym Sci 2008, 107, 3058.
16. Romero-Guzmán, M. E.; Romo-Uribe, A.; Zárate-Hernández, B. M.; Cruz-Silva, R. Rheol Acta 2009, 48, 641.
17. Dorigato, A.; Pegoretti, A.; Migliaresi, C. J Appl Polym Sci 2009, 114, 2270.
18. Zhou, Z.; Yin, N.; Zhan, Y.; Zhang, Y. J Appl Polym Sci 2008, 107, 825.
19. Zhou, Z.; Zhang, Y.; Zhang, Y.; Yin, N. J Polym Sci Part B: Polym Phys 2008, 46, 526.
20. Kim, H. U.; Bang, Y. H.; Choi, S. M.; Yoon, K. H. Compos Sci Technol 2008, 68, 2739.
21. Signori, F.; Coltelli, M. B.; Bronco, S. Polym Degrad Stab 2009, 94, 74.
22. Migliaresi, C. D.; Cohn, D.; De Lollis, A.; Fambri, L. J Appl Polym Sci 1991, 43, 83.
23. Pan, P.; Liang, Z.; Zhu, B.; Dong, T.; Inoue, Y. Macromolecules 2008, 41, 8011.
24. Constantinos, T.; Bokaris, E. P. Polym Bull 1993, 30, 609.
25. Lewitus, D.; McCarthy, S.; Ophir, A.; Kenig, S. J Polym Environ 2006, 14, 171.